A Tropospheric Ozone Maximum Over the Middle East

Qinbin Li, Daniel J. Jacob, Jennifer A. Logan, Isabelle Bey, Robert M. Yantosca, Hongyu Liu, Randall V. Martin, Arlene M. Fiore, Brendan D. Field, and Bryan N. Duncan

Department of Earth & Planetary Sciences and Division of Engineering & Applied Sciences, Harvard University, Cambridge, Massachusetts

Valérie Thouret

Laboratoire d'Aérologie CNRS (UMR 5560), Toulouse, France

Abstract. The GEOS-CHEM global 3-D model of tropospheric chemistry predicts a summertime O_3 maximum over the Middle East, with mean mixing ratios in the middle and upper troposphere in excess of 80 ppbv. This model feature is consistent with the few observations from commercial aircraft in the region. Its origin in the model reflects a complex interplay of dynamical and chemical factors, and of anthropogenic and natural influences. The anticyclonic circulation in the middle and upper troposphere over the Middle East funnels northern midlatitude pollution transported in the westerly subtropical jet as well as lightning outflow from the Indian monsoon and pollution from eastern Asia transported in an easterly tropical jet. Large-scale subsidence over the region takes place with continued net production of O_3 and little mid-level outflow. Transport from the stratosphere does not contribute significantly to the O_3 maximum. Sensitivity simulations with anthropogenic or lightning emissions shut off indicate decreases of 20-30% and 10-15% respectively in the tropospheric O_3 column over the Middle East. More observations in this region are needed to confirm the presence of the O_3 maximum.

Introduction

The GEOS-CHEM global 3-D model of tropospheric chemistry [*Bey et al.*, 2001] predicts a summer O_3 maximum in the middle troposphere over the Middle East (Figure 1, left panel). This maximum is also seen in the simulated tropospheric O_3 column (Figure 1, right panel). The Middle East is a largely unexplored region for O_3 observations, but vertical profiles from the MOZAIC program on commercial aircraft [*Marenco et al.,* 1998; *Stohl et al.,* 2001] indicate high summer mixing ratios that are comparable to model values (Figure 1 and Figure 2). Tropospheric O_3 columns in July simulated with GEOS-CHEM are usually within 10% of values observed in the MOZAIC and ozonesonde data. The Middle East maximum in the model appears in May and disappears in September, consistent with the MOZAIC data (Figure 2).

Several global 3-D models of tropospheric chemistry have been described in the recent literature, but only a few have published documentations on their global O_3 distributions in

the free troposphere in summer. *Hauglustaine et al.* [1998] find a maximum in the tropospheric O_3 column over the Middle East in September-October. *Wang et al.* [1998b] and *Mickley et al.* [1999] show a broad Eurasian maximum in summer. *Jonson et al.* [2001] show high values (>90 ppbv) at 500 hPa over the Middle East in July, but even higher values at northern midlatitudes. *Horowitz et al.* [2001] show a 500 hPa O_3 maximum over the Middle East in July.

We examine here the origin of the Middle East O_3 maximum simulated by the GEOS-CHEM model. This origin is not obvious, and its confirmation or rejection by more detailed observations of O_3 in the future will provide an important test of our understanding of tropospheric chemistry. An anthropogenic origin for this maximum would have important implications for radiative forcing of climate [*Mickley et al.*, 1999].

Model Description and Simulation of the Middle East Ozone Maximum

The GEOS-CHEM model is driven by assimilated meteorological data from the Goddard Earth Observing System (GEOS) of the NASA Data Assimilation Office (DAO) [*Schubert et al.*, 1993]. We use meteorological fields for 1993-1997 provided at 3- and 6-hour frequencies with horizontal resolution of 4° latitude by 5° longitude and with 20 (1993-1995) or 26 (1996-1997) σ layers in the vertical between the Earth's surface and 10 hPa (1993-1995) or 0.1 hPa (1996-1997). Simulation of O_3 in the model uses a chemical mechanism with 120 species to describe tropospheric O_3-NO_x-hydrocarbon chemistry. A detailed description and evaluation of the model is given by *Bey et al.* [2001].

Anthropogenic emissions are specified using a base emission inventory for 1985 scaled to 1993-1995 following *Bey et al.* [2001]. The base inventory includes NO_x emissions from *Benkovitz et al.* [1996], nonmethane hydrocarbon (NMHC) emissions from *Piccot et al.* [1992] and CO emissions as summarized in *Wang et al.* [1998a]. Lightning NO_x emissions are linked to deep convection following the parameterization of *Price and Rind* [1992]. The resulting anthropogenic and lightning sources of NO_x are 22.8 $Tg\,N\,yr^{-1}$ and 3.4 $Tg\,N\,yr^{-1}$, respectively. The cross-tropopause transport of O_3 is simulated by the Synoz method of *McLinden et al.* [2000] with a global cross-tropopause flux of 475 $Tg\,O_3\,yr^{-1}$.

We conducted a five-year simulation for 1993-1997. The interannual variations in the 400 hPa O_3 mixing ratios and tropospheric O_3 columns averaged over the Middle East in
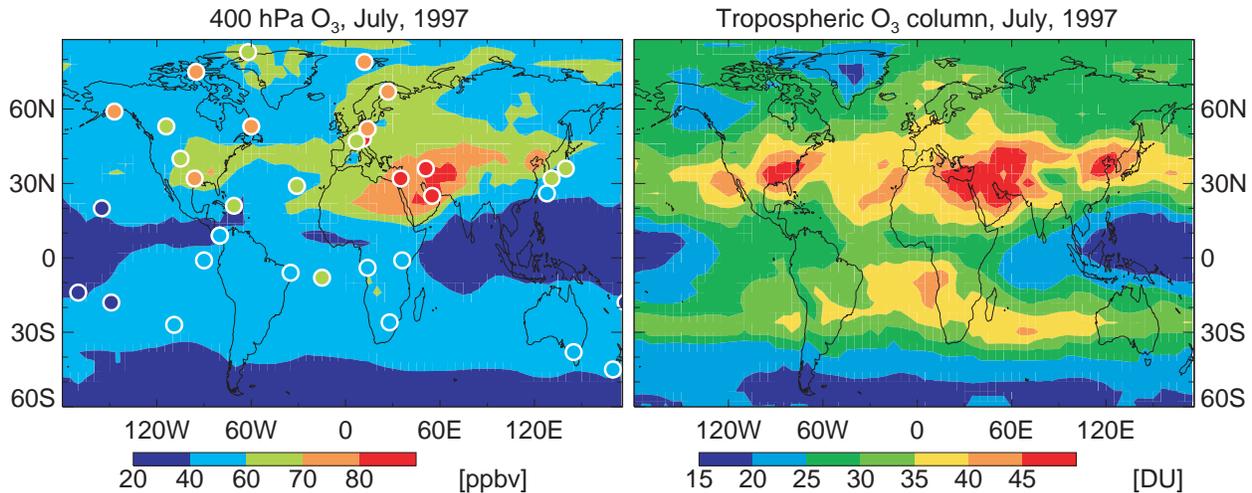
Figure 1. Simulated monthly mean O_3 in July 1997. Left panel: 400 hPa mixing ratios (ppbv). Right panel: tropospheric columns in Dobson units (1 DU = 2.69×10^{16} molecules cm^{-2}). Colored circles in the left panel show measured monthly mean O_3 mixing ratios at 400 hPa in July including climatological ozonesonde data [*Logan,* 1999], and values from commercial aircraft over Tel-Aviv (32°N, 35°E), Dubai (25°N, 55°E), and Teheran (36°N, 51°E) during 1995-2000 as part of the MOZAIC program.

July are less than 5%. All five years feature the Middle East maximum. Our analysis focuses on July 1997. Sensitivity simulations are initialized in March 1997; earlier initialization has little effect on results.

Figure 3 shows the O_3 fluxes and production rates at 250 hPa (left panel) and the O_3 fluxes at 500 hPa (right panel). In summer, the meteorological setting over the Middle East is dominated by a heat low at the surface and an anticyclonic circulation in the middle and upper troposphere with large-scale subsidence [*Takahashi and Arakawa,* 1981; *Ye and Wu,* 1998]. In the north of the region, circumpolar transport of O_3 takes place in the westerly subtropical jet centered at 40°N (Figure 3). Much of the O_3 at northern midlatitudes is of anthropogenic origin. Entrainment of this midlatitude pollution into the anticyclonic circulation over the Middle East is apparent below 400 hPa (Figure 3, right panel). In the lower troposphere, the prevailing summer northwesterlies over the eastern Mediterranean [*Dayan,* 1986] transport anthropogenic O_3 from Europe into the Middle East and northern Africa.

The left panel of Figure 3 indicates easterly transport at high altitudes of O_3 produced in the upper troposphere over southern and eastern Asia. Intense lightning associated with the summer monsoon produces large amounts of NO_x in the upper troposphere over the Indian subcontinent [*Christian and Latham,* 1998; *Nesbitt et al.,* 2000], while strong convection over eastern Asia transports large amounts of anthropogenic NO_x to the upper troposphere. The model simulates 0.20-0.24 ppbv NO_x in the upper troposphere over the Indian subcontinent, similar to the levels of NO_x observed by commercial aircraft over that region [*Brunner et al.,* 1998]. Simulated O_3 production rates in the upper troposphere over southern and eastern Asia exceed 5 ppb day^{-1} (Figure 3, left panel), an unusually high value [*Jaeglé et al.,* 2001]. The resulting O_3 is transported to the Middle East by the tropical easterly jet as part of the anticyclonic circulation over South Asia (Figure 3, left panel). The easterly flow in the upper troposphere at 20-30°N is a well-known feature of the summertime South Asia circulation [*Takahashi and Arakawa,* 1981; *Ye and Wu,* 1998].

We analyzed the model budget of tropospheric O_3 for the Middle East region defined as the rectangle in the right panel of Figure 3. Net inflow through the eastern boundary of the region accounts for 65% of the regional O_3 supply to the upper troposphere (<300 hPa) while *in situ* chemical production provides another 30%. Downward transport from the stratosphere is unimportant. Net O_3 production takes place above 500 hPa (~6 km) and in the boundary layer up to 700 hPa (2-3 km). In the upper troposphere, the production is driven primarily by lightning NO_x advected into the region from the Indian monsoon, while in the boundary layer it is driven by local anthropogenic NO_x. Subsidence from the upper troposphere provides 80% of the O_3 supply to the middle troposphere in the region, sustaining the O_3 maximum. Upward transport takes place in the lower
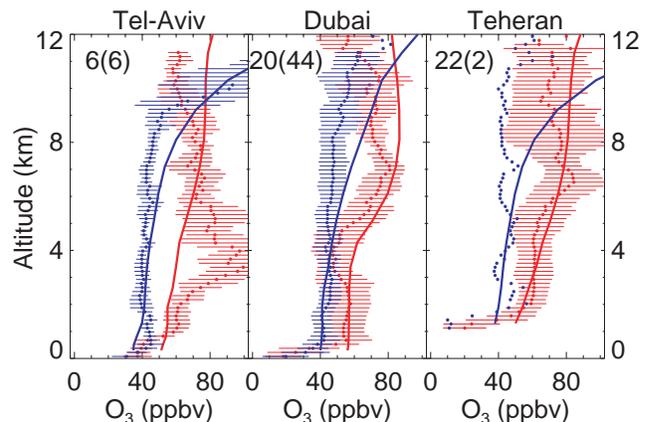

Figure 2. Monthly mean January (blue) and July (red) O_3 vertical profiles over Tel-Aviv, Dubai, and Teheran. Solid lines are model results. Observations during 1995-2000 from the MOZAIC program are shown as dotted lines with standard deviations indicated. The number of observed profiles are indicated by the two numbers with the first one for July and the second one for January. The elevated O_3 at 2-4 km over Tel-Aviv in the observations is due to European influence.
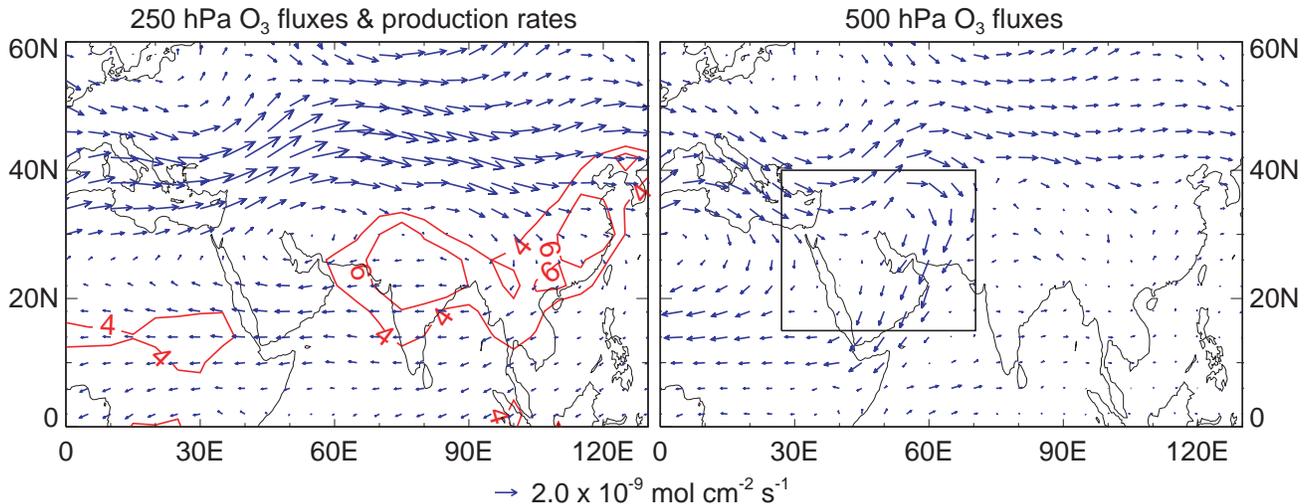
Figure 3. Simulated horizontal O_3 fluxes (arrows) and net chemical O_3 production rates (contours, $> 4 \, \mathrm{ppb \, day^{-1}}$) at 250 hPa (left panel) and horizontal O_3 fluxes at 500 hPa (right panel). Values are model monthly means for July 1997. The rectangle in the right panel indicates the Middle East region used for budget analysis.

troposphere due to convection and convergence associated with the surface heat low. Removal of O_3 from the region is mostly by outflow to the Indian Ocean and to the Sahara at about 700 hPa.

Sources Contributing to the Ozone Maximum

We used tagged O_3 (odd oxygen) tracers [*Wang et al.,* 1998c] and sensitivity simulations to further understand the geographical source regions and precursor emissions contributing to the Middle East maximum. The tagged tracer simulation transports as separate tracers O_3 originating in the stratosphere, upper troposphere (<300 hPa), middle troposphere (300-600 hPa) and the lower troposphere (>600 hPa). We find that production in the upper and middle troposphere accounts for 30-40 ppbv (35-50%) and 10-20 ppbv (15-25%) respectively of the 400 hPa O_3 over the Middle East, while production in the lower troposphere and transport from the stratosphere account for 15-20 ppbv (20-25%) and less than 10 ppbv (15%), respectively. The particularly high contribution of upper tropospheric production to O_3 over the Middle East, relative to other regions in the northern subtropical band, reflects the large-scale subsidence over the region. Although the overall contribution from the stratosphere is relatively small, it is higher over the Middle East than over other northern subtropical regions.

To determine the relative contributions to the O_3 maximum from anthropogenic versus lightning emissions, we conducted sensitivity simulations with either anthropogenic or lightning emissions or both omitted. We also conducted simulations in which anthropogenic emissions from the Middle East, Asia (not including the Middle East), Europe, and North America were omitted separately. Figure 4 shows the differences in the simulated tropospheric O_3 columns and 400 hPa O_3 mixing ratios relative to the standard simulation. Suppressing lightning emissions decreases the O_3 column over the Middle East in July by 5-7 DU (10-15%), while suppressing anthropogenic emissions leads to a 8-12 DU (20-30%) decrease (Figures 4a,c). The effects of light-
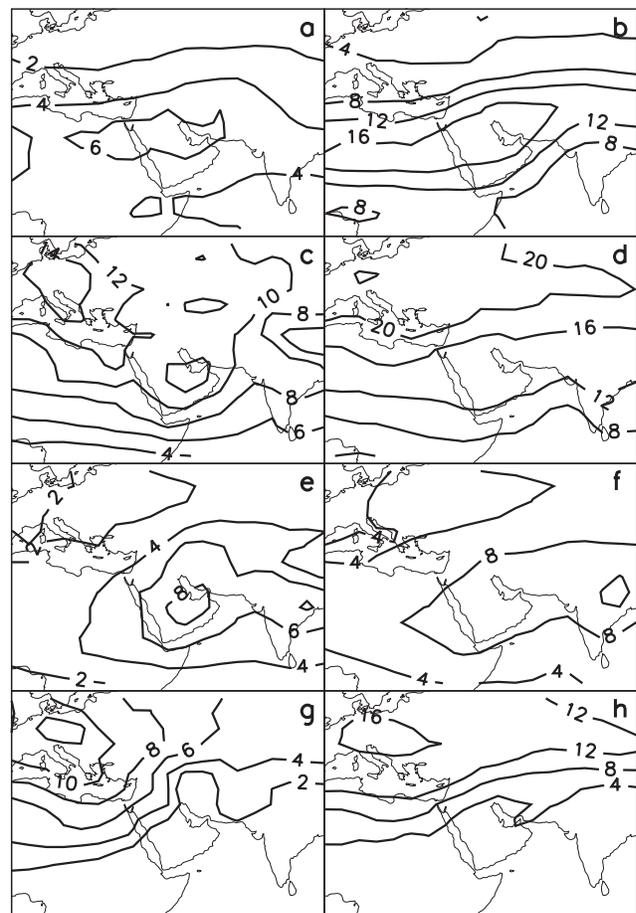

Figure 4. Decreases in simulated monthly mean tropospheric O_3 columns (left panels, in DU) and 400 hPa O_3 mixing ratios (right panels, in ppbv) over the Middle East in July 1997 when (a,b) lightning (c,d) anthropogenic (e,f) Asian anthropogenic (g,h) North American and European anthropogenic emissions are suppressed, relative to the standard simulation.

ning and anthropogenic emissions on the tropospheric O_3 column both show maxima in the Middle East, because of the strong subsidence over the region as discussed previously. Lightning and anthropogenic emissions each contribute 10-20 ppbv to the 400 hPa O_3 over the Middle East (Figures 4b,d). The effect of suppressing both lightning and anthropogenic emissions is found to be nearly additive; even with these two sources suppressed there remains a Middle East maximum (peaking at 47 ppbv at 400 hPa) because of subsidence.

Further investigation of the anthropogenic influence on the Middle East maximum indicates that Asian influence dominates in the southern part of the region, while European and North American influences dominate in the north, reflecting the flow patterns described previously (Figures 4e-h). European and North American influences are found to be of comparable magnitudes. The column maximum in Figure 4e is mainly due to local emissions, while the mixing ratio maximum at 400 hPa in Figure 4f is due largely to emissions from southern and eastern Asia.

The summertime troposphere O_3 maximum simulated by the GEOS-CHEM model over the Middle East thus reflects a complex interplay of transport and chemistry as well as a superimposition of anthropogenic and natural (lightning) influences. More observations are needed to confirm the presence and intensity of this maximum, and would provide an important test for the current understanding of tropospheric O_3 chemistry. Satellite observations would be particularly valuable.

References

Benkovitz, C. M. et al., Global gridded inventories for anthropogenic emissions of sulfur and nitrogen, *J. Geophys. Res., 101,* 29,239-29,253, 1996.

Bey, I. et al., Global modeling of tropospheric chemistry with assimilated meteorology: Model description and evaluation, *J. Geophys. Res.,* in press, 2001.

Brunner, D., J. Staehelin, D. Jeker, Large-scale nitrogen oxide plumes in the tropopause region and implications for ozone, *Science, 282,* 1305-1309, 1998.

Christian, H. J., and J. Latham, Satellite measurements of global lightning, *Q. J. R. Meteorol. Soc., 124,* 1771-1773, 1998.

Dayan, U., Climatology of back trajectories from Israel based on synoptic analysis, *J. Clim. Appl. Meteorol., 25,* 591-595, 1986.

Hauglustaine, D. A. et al., MOZART, a global chemical transport model for ozone and related chemical tracers 2. Model results and evaluation, *J. Geophys. Res., 103,* 28,291-28,335, 1998.

Horowitz, L. W. et al., A global simulation of tropospheric ozone and related tracers: Description and evaluation of MOZART, Ver. 2, *Eos. Trans. AGU, 82*(20), S39, 2001.

Jaeglé, L., D. J. Jacob, W. H. Brune, and P. O. Wennberg, Chemistry of HO_x radicals in the upper troposphere, *Atmos. Environ., 35,* 469-489, 2001.

Jonson, J. E., J. K. Sundet, and L. Tarrasón, Model calculations of present and future levels of ozone and ozone precursors with a global and a regional model, *Atmos. Environ., 35,* 525-537, 2001.

Logan, J., An analysis of ozonesonde data for the troposphere: Recommendations for testing 3-D models and development of a gridded climatology for tropospheric ozone, *J. Geophys. Res., 104,* 16,115-16,149, 1999.

Marenco, A., et al., Measurement of ozone and water vapor by Airbus in-service aircraft: The MOZAIC airborne program, An overview, *J. Geophys. Res., 103,* 25,631-25,642, 1998.

McLinden, C. A. et al., Stratospheric ozone in 3-D models: A simple chemistry and the cross-tropopause flux, *J. Geophys. Res., 105,* 14,653-14,665, 2000.

Mickley, L. J. et al., Radiative forcing from tropospheric ozone calculated with a unified chemistry-climate model, *J. Geophys. Res., 104,* 30,153-30,172, 1999.

Nesbitt, S. W., R. Zhang, and R. E. Orville, Seasonal and global NO_x production by lightning estimated from the Optical Transient Detector (OTD), *Tellus, 52B,* 1206-1215, 2000.

Olivier, J. G. et al., Emission Database for Global Atmospheric Research (EDGAR), *Environ. Monit. Assessment, 31,* 93-106, 1994.

Piccot, S. D., J. J. Watson, and J. W. Jones, A global inventory of volatile organic compound emissions from anthropogenic sources, *J. Geophys. Res., 97,* 9897-9912, 1992.

Price, C., and D. Rind, A simple lightning parameterization for calculating global lightning distributions, *J. Geophys. Res., 97,* 9919-9933, 1992.

Schubert, S. D., R. B. Rood, and J. Pfaendtner, An assimilated data set for Earth Science applications, *Bull. Am. Meteorol. Soc., 74,* 2331-2342, 1993.

Stohl, A. et al., An extension of MOZAIC ozone climatologies using trajectory statistics, *J. Geophys. Res.,* submitted, 2001.

Takahashi, T., and H. Arakawa, Climates of Southern and Western Asia, *World Survey of Climatology, Vol. 9,* Elsevier Scientific Publishing Co., New York, 1981.

Wang, Y., D. J. Jacob, and J. A. Logan, Global simulation of tropospheric O_3-NO_x-hydrocarbon chemistry 1. Model formulation, *J. Geophys. Res., 103,* 10,713-10,725, 1998a.

Wang, Y., J. A. Logan, and D. J. Jacob, Global simulation of tropospheric O_3-NO_x-hydrocarbon chemistry 2. Model evaluation and global ozone budget, *J. Geophys. Res., 103,* 10,727-10,755, 1998b.

Wang, Y., D. J. Jacob, and J. A. Logan, Global simulation of tropospheric O_3-NO_x-hydrocarbon chemistry 3. Origin of tropospheric ozone and effects of nonmethane hydrocarbons, *J. Geophys. Res., 103,* 10,757-10,767, 1998c.

Ye, D., and G. Wu, The role of the heat source of the Tibetan plateau in the gerneral circulation, *Meteorol. Atmos. Phys., 67,* 181-198, 1998.